

# Loading indirect excitons into an electrostatic trap formed in coupled GaAs quantum wells

A. Gärtner<sup>a</sup>, D. Schuh<sup>b,c</sup>, A.W. Holleitner<sup>c,a,\*</sup>, J.P. Kotthaus<sup>a</sup>

<sup>a</sup>Center for NanoScience (CeNS), Ludwig-Maximilians-University Munich, Geschwister-Scholl-Platz 1, 80539 Munich, Germany

<sup>b</sup>Institut für Angewandte Physik und Experimentelle Physik, Universität Regensburg, Universitätsstraße 31, 93040 Regensburg, Germany

<sup>c</sup>Walter Schottky Institut, Technische Universität München, Am Coulombwall 3, 85748 Garching, Germany

Available online 23 October 2007

## Abstract

We demonstrate how to load indirect excitons into an electrostatic trap, which is formed in a field-effect structure based on coupled GaAs quantum wells. Within the plane of a double quantum well, indirect excitons are trapped at the perimeter of a SiO<sub>2</sub> area sandwiched between the surface of the GaAs heterostructure and a semi-transparent metallic top gate. The trapping mechanism is well explained by a combination of the quantum confined Stark effect and local field enhancement. We find that the trap can be filled with indirect excitons, as soon as the distance between the laser excitation and the trap is shorter than the effective diffusion length of the indirect excitons.

© 2007 Elsevier B.V. All rights reserved.

PACS: 71.35.-y; 71.35.Lk; 78.55.Cr

Keywords: Excitons; III–V Semiconductors; Low-dimensional system; Double quantum wells

In 1968, Keldysh and Kozlov [1] predicted the possibility of a Bose–Einstein condensation of excitons in solid state systems. For detecting the Bose–Einstein condensation of excitons, it is a prerequisite to define controllable confinement potentials for excitons. So far, trapping of excitons has been demonstrated in “natural traps” defined by interface roughness fluctuations [2], in magnetic traps [3], in strained systems [4–6], and electrostatic traps [7–13]. Recently, we reported on a novel electrostatic trap for indirect excitons in a GaAs double quantum well heterostructure [14]. The indirect excitons are trapped in GaAs quantum wells just below the perimeter of SiO<sub>2</sub> layers, which are sandwiched between the surface of the GaAs heterostructure and a semi-transparent metallic top gate. The trapping mechanism relies on a local electrostatic field enhancement in combination with the quantum confined Stark effect [15]. We found that the trap gives rise to a very steep harmonic trapping potential with an effective spring-constant of up to 11 keV/cm<sup>2</sup> [14]. Here, we report on the

loading characteristics of such an electrostatic trap. We find that the trap can be filled with indirect excitons, when the excitons are optically excited at a horizontal distance of approximately 50–70 μm away from the trap. The distance equals approximately the diffusion length of the indirect excitons. For shorter distances, the trap is loaded with “hot” excitons, which finally spill out from the trap due to excess energy. For distances longer than the exciton diffusion length, the traps are not filled with excitons, and they appear dark.

Starting point is an epitaxially grown AlGaAs/GaAs heterostructure, which contains two GaAs quantum wells encompassed by Al<sub>0.3</sub>Ga<sub>0.7</sub>As barriers (see Fig. 1a). Each quantum well has a thickness of 8 nm, and the quantum wells are separated by an Al<sub>0.3</sub>Ga<sub>0.7</sub>As tunnel barrier with a thickness of 4 nm. The centers of the double quantum wells are located 60 nm below the surface of the heterostructure. An n-doped GaAs layer at a depth (*d*) of 370 nm serves as a back gate, while a semi-transparent titanium layer is used as the top gate of the field-effect device. In this structure, electrons and holes of photogenerated excitons may rearrange in a way that they are spatially separated by

\*Corresponding author. Tel.: +49 89 28912775; fax: +49 89 3206620.  
E-mail address: [holleitner@wsi.tum.de](mailto:holleitner@wsi.tum.de) (A.W. Holleitner).

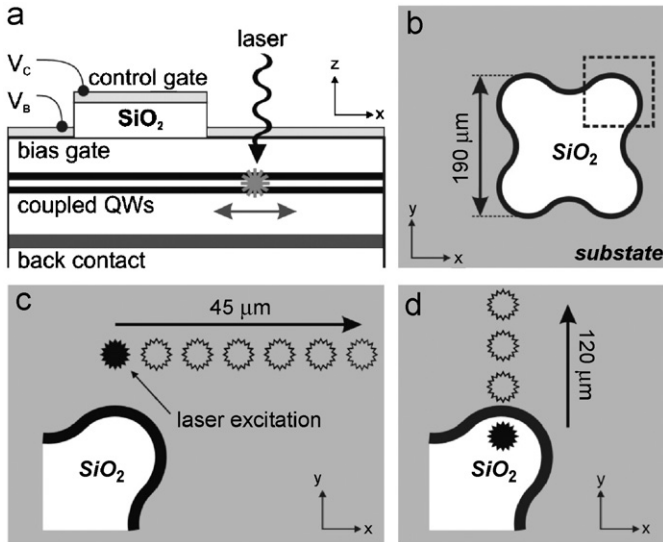


Fig. 1. Schematic side view (a) and top view (b) of the field-effect structure with an additional  $\text{SiO}_2$  layer on top of the GaAs/AlGaAs heterostructure. Indirect, long-living excitons are laser-generated in the coupled quantum wells (QWs). By appropriately tuning the bias voltage  $V_B$  and the control voltage  $V_C$  with respect to the back gate, excitons can be captured and stored along the circumference of the  $\text{SiO}_2$  layers with varying curvature [14], such as a shamrock sketched in part (b). In order to unveil the photoluminescence characteristics of the traps as a function of the distance of the laser excitation to the trap, the excitation spot is moved laterally across the sample, either in  $x$ -direction (c) or in  $y$ -direction (d). Both part (c) and part (d) show magnified representations of the dashed region in part (b).

the tunnel barrier between the GaAs quantum wells [16]. The lifetime of such indirect excitons is voltage-tunable via the top gate [16,17] and reaches values of up to  $30 \mu\text{s}$  [18]. In contrast, the optical lifetime of direct excitons in quantum wells is shorter than 1 ns (for  $T = 5 \text{ K}$ ) [15]. As depicted in Fig. 1a and b, the investigated samples feature an additional  $\text{SiO}_2$  layer, which is sandwiched between the GaAs surface and the metal top gate. The thickness of the  $\text{SiO}_2$  layer is about 50 nm, and the titanium top gate has a thickness of about 10 nm. The top gate can be distinguished in two regions: the bias gate, which is in direct contact with the GaAs heterostructure, and the control gate, which is located on top of the  $\text{SiO}_2$  layer. As there is no electrical connection between the bias gate and the control gate, the two regions can be tuned independently to different voltages  $V_B$  and  $V_C$ , respectively [14,15]. However, for the experiments reported in this article, the bias gate was grounded ( $V_B = 0 \text{ V}$ ) and the control gate was floating. All experiments on exciton trapping and storage are carried out in a continuous-flow helium cryostat at a temperature of 3.7 K in combination with a time-resolved micro-photoluminescence setup. The excitons are locally excited within the coupled quantum wells by focusing a pulsed laser with a wavelength of 680 nm onto the sample (Fig. 1a). The laser is operated at a pulse length of 50 ns, and the repetition period is set to be  $10 \mu\text{s}$ . The laser beam is focused to a spot with a diameter of  $10 \mu\text{m}$  with a typical power density of  $5 \text{ kW/cm}^2$ . The photoluminescence signal

of the recombining excitons is collected by the optical microscope after a delay of 800 ns with regard to the initial laser pulse. By this delay period, which can be interpreted as the exciton storage time, we assure that only long-living, indirect excitons are subject to the measurements. The optical photoluminescence signal is detected with a lateral resolution of  $\sim 2 \mu\text{m}$  using a fast-gated, intensified charge-coupled device (ICCD) camera with an exposure time of 50 ns. In order to obtain a sufficient signal-to-noise ratio, the experiments are performed by integrating over  $4 \times 10^6$  single events [15].

Fig. 1c and d depict the experimental scheme. The photoluminescence emission from samples with a  $\text{SiO}_2$  layer is measured as a function of the distance between the laser excitation and the exciton trap. In Fig. 1c, the laser is moved along the  $x$ -direction coinciding with the crystal's [110] direction. An analogous movement along the  $y$ -direction, representing the  $[\bar{1}10]$  direction, is shown in Fig. 1d. In Fig. 2a–f, the spatially resolved photoluminescence signal from an electrostatic trap is depicted, while the laser spot is moved in steps of approximately  $24 \mu\text{m}$  by a total distance of  $120 \pm 5 \mu\text{m}$  in the  $y$ -direction. In Fig. 3a–f, a similar measurement is performed for the  $x$ -direction, at a step size of approximately  $9 \mu\text{m}$ , and a total translational distance of  $45 \pm 5 \mu\text{m}$ . Please note that the set of figures shown in Fig. 2 share a common gray scale for the intensity (same applies for Fig. 3). We find in both Figs. 2 and 3 that the photoluminescence of the trap decreases to 0 for a radial distance  $r \geq 70 \mu\text{m}$  between the excitation spot and the trap. In addition, we see that for  $r \leq 50 \mu\text{m}$  the photoluminescence signal is constant at a high value. Only

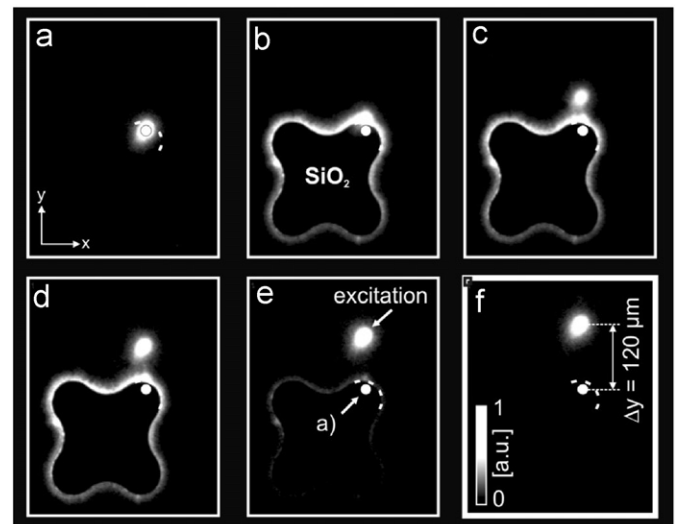


Fig. 2. (a–f) The spatial photoluminescence signal of a trap is detected as a function of the distance between the laser excitation and the exciton trap at 3.7 K. The photoluminescence is recorded using a band-pass filter in order to reduce the signal originating from direct excitons and carbon defect sites [15]. The laser is moved along the  $y$ -direction with respect to the trap (see Fig. 1), i.e. along the [110] direction of the crystal. In parts (b–f), the location of the excitation spot used in part (a) is given as a reference (white circle).

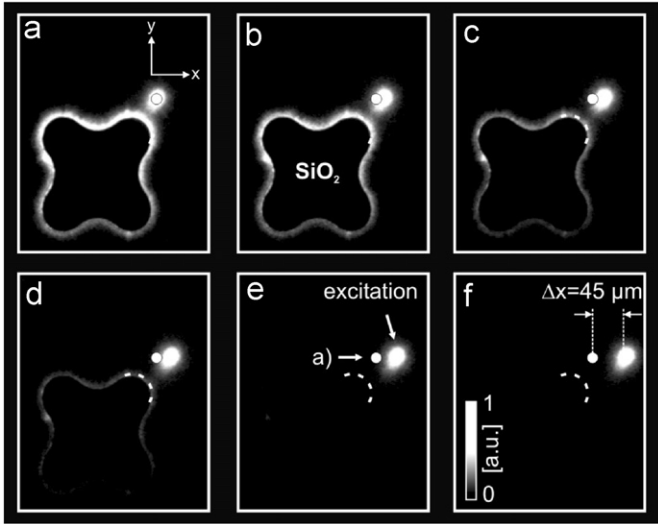


Fig. 3. (a–f) Spatial photoluminescence signal as a function of the distance between the laser excitation and the exciton trap. The laser spot is moved along the  $x$ -direction at 3.7 K. In parts (b–f), the location of the excitation spot used in part (a) is given as a reference (white circle).

for  $50 \mu\text{m} \leq r_0 \leq 70 \mu\text{m}$ , the photoluminescence signal depends significantly on the radial distance  $r$  (e.g. Figs. 2e, 3c and d).

It is reasonable to assume that this radial distance agrees with the diffusion length of the indirect excitons in a field-effect structure as depicted in Fig. 1. We determined an upper limit of the diffusion coefficient ( $D$ ) to be  $30 \text{ cm}^2/\text{s}$  [16]. Hereby, we can estimate the diffusion displacement of the indirect excitons to be  $(2 \times D \times \tau)^{1/2} = (2 \times 30 \text{ cm}^2/\text{s} \times 800 \text{ ns})^{1/2} \sim 70 \mu\text{m}$  [18], which is in reasonable agreement with  $r_0$ . However, we would like to note that it is well known for indirect excitons in coupled GaAs quantum wells that immediately after the laser pulse ( $< 1 \text{ ns}$ ), the cloud of indirect excitons expands rapidly, and only at later times, a comparably slow linear diffusion process can be assumed [18]. The quick initial expansion is usually explained by the exciton dipole–dipole repulsion at high exciton densities, and a filling effect of the local minima in the energy landscape of the quantum wells [19]. Experimentally, we find that the variance of the exciton distribution saturates at a distance of  $50\text{--}70 \mu\text{m}$  for delay times longer than  $\sim 200 \text{ ns}$ , as was also reported in Ref. [18]. Hereby, we assume that this distance is the effective diffusion length of the exciton system at  $800 \text{ ns}$  in our sample. As a result, we interpret the experimental findings of Figs. 2 and 3 as follows (Fig. 4). For a distance longer than  $r_0$ , the main part of the optically excited indirect excitons does not diffuse to the traps, and the traps appear dark (Figs. 2f and 3e,f). At a distance  $\sim r_0$ , the traps start to fill up with long-living indirect excitons (Figs. 2e, 3c,d). This distance is the most appropriate distance to load the trap with thermally equilibrated excitons. During the diffusion, the excitons can scatter at acoustic phonons and impurities such that they equilibrate to the lattice temperature. For distances  $r$  shorter than  $r_0$ , the traps are completely filled with indirect excitons up to

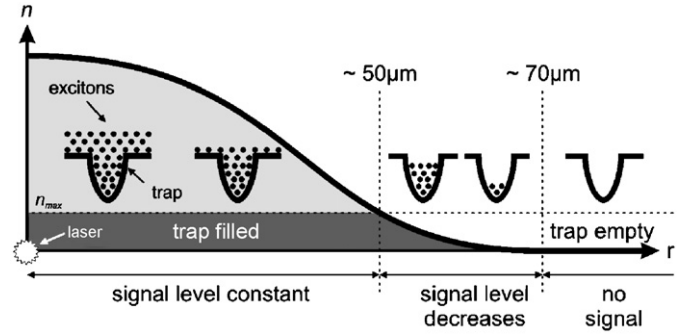


Fig. 4. Sketch of the exciton density ( $n$ ) as a function of the radial distance ( $r$ ) measured from the trap to the position of the initial laser excitation. The latter is indicated at the left side of the graph. For a distance  $r \leq 50 \mu\text{m}$ , the traps are completely filled to the density  $n_{\text{max}}$  and spill over. For  $50 \leq r \leq 70 \mu\text{m}$ , the traps are only partially filled, yielding a position-dependent photoluminescence signal that decreases with increasing distance  $r$ . For  $r \geq 70 \mu\text{m}$ , the traps are completely empty, and they appear dark.

the trap’s maximum density  $n_{\text{max}}$  (Figs. 2b–d and 3a,b). Hereby, the trap spills over due to dipole–dipole repulsion of the excitons. As a result, the trap has a constant photoluminescence signal for  $r < r_0$ . Please note that the trap is not loaded with excitons at all in case the laser excitation takes place at the  $\text{SiO}_2$  covered area (Fig. 2a), as we recently reported in Refs. [14,15].

To estimate the corresponding exciton density  $n_{\text{max}}$  within the trap, we measure the blue-shift of the exciton photoluminescence as a function of the laser power which translates directly to the excitonic density [15]. The high-density limit is established experimentally in the regime of constant photoluminescence intensity (e.g. Figs. 2b and 3a). The low-density limit is yielded by a low-power excitation at the same lateral position (data not shown). The blue-shift is determined to be  $\sim 5 \text{ meV}$  corresponding to an excitonic density in the range of  $n_{\text{max}} \sim 10^9$  to  $10^{10} \text{ cm}^{-2}$  [15].

In summary, we report on the successful loading of indirect excitons into an electrostatically tunable trap at reasonably high densities. The steep confinement potential for excitons in conjunction with the in situ tunability of the trap promotes the technique to a promising candidate for future experiments on Bose–Einstein condensation of excitons in solid state systems. Future work aims towards realizing traps that confine excitons in all three spatial dimensions.

We gratefully acknowledge financial support by the Grant KO-416/17 of the Deutsche Forschungsgemeinschaft (DFG), the Center for NanoScience (CeNS) in Munich, and the German excellence initiative via the cluster “Nanosystems Initiative Munich (NIM)”.

## References

- [1] L.V. Keldysh, A.N. Kozlov, Sov. Phys. JETP 27 (1968) 521.
- [2] L.V. Butov, C.W. Lai, A.L. Ivanov, A.C. Gossard, D.S. Chemla, Nature 417 (2002) 47.

- [3] P.C.M. Christianen, F. Piazza, J.G.S. Lok, J.C. Maan, W. van der Vleuten, *Physica B* 249 (1998) 624.
- [4] D.P. Trauernicht, A. Mysyrowicz, J.P. Wolfe, *Phys. Rev. B* 28 (1983) 3590.
- [5] K. Kash, J.M. Worlock, M.D. Sturge, P. Grabbe, J.P. Harbison, A. Scherer, P.S.D. Lin, *Appl. Phys. Lett.* 53 (1988) 782.
- [6] V. Negotia, D.W. Snoke, K. Eberl, *Appl. Phys. Lett.* 75 (1999) 2059.
- [7] M. Hagn, A. Zrenner, G. Bohm, G. Weimann, *Appl. Phys. Lett.* 67 (1995) 232.
- [8] S. Zimmermann, A.O. Govorov, W. Hansen, J.P. Kotthaus, M. Bichler, W. Wegscheider, *Phys. Rev. B* 56 (1997) 13414.
- [9] T. Huber, A. Zrenner, W. Wegscheider, M. Bichler, *Phys. Status Solidi (a)* 166 (1998) R5.
- [10] J. Krauß, et al., *Phys. Rev. Lett.* 88 (2002) 036803.
- [11] T. Hammack, N.A. Gippius, G.O. Andreev, L.V. Butov, M. Hanson, A.C. Gossard, *J. Appl. Phys.* 99 (2006) 066104.
- [12] J.P. Kotthaus, *Phys. Status Solidi (b)* 243 (2006) 3754.
- [13] R. Rapaport, G. Chen, S. Simon, O. Mitrofanov, L. Pfeiffer, P.M. Platzman, *Phys. Rev. B* 72 (2005) 075428.
- [14] A. Gärtner, L. Prechtel, D. Schuh, A.W. Holleitner, J.P. Kotthaus, *Phys. Rev. B* 76 (2007) 085304.
- [15] A. Gärtner, *Dynamik von Exzitonen in elektrostatisch definierten Potentiallandschaften*, Dr. Hut Verlag, München, 2006. ISBN 978-3899-63464-8.
- [16] A. Gärtner, A.W. Holleitner, J.P. Kotthaus, D. Schuh, *Appl. Phys. Lett.* 89 (2006) 052108.
- [17] A. Gärtner, D. Schuh, J.P. Kotthaus, *Physica E* 32 (2006) 195.
- [18] Z. Vörös, R. Balili, D.W. Snoke, L. Pfeiffer, K. West, *Phys. Rev. Lett.* 94 (2005) 226401.
- [19] A.L. Ivanov, *Europhys. Lett.* 59 (2002) 586.